

# EXPERIMENTAL STUDY OF THE ELECTRON BEAM PRODUCED BY A PLASMA FOCUS ACCELERATOR\*

R. F. Schneider, M. J. Rhee, and J. R. Smith<sup>a)</sup>

Laboratory for Plasma and Fusion Energy Studies  
University of Maryland  
College Park, Maryland 20742

## Abstract

The electron beam produced by a compact pulsed plasma focus accelerator is investigated. In the prototype device, 5-20 ns electron beam pulses of several kA and particle energies of up to a few hundred keV have been produced. The rms emittance is found to be 1288 mm-mrad.

## I. Introduction

In recent years the electron beam produced by the plasma focus has proven quite attractive for such a compact device.<sup>1-8</sup> A theoretical description of the phenomenon, however, has been quite difficult to develop. Simple lumped circuit models of the plasma focus have been some utility in describing elementary aspects such as current flow through the plasma up to the onset of the focus instability<sup>9,10</sup> at which time the model breaks down. A simple transmission line theory has been proposed<sup>11</sup> which may explain certain aspects of the output pulse, i.e. voltage, current, and duration. Unfortunately a full understanding of the focus instability has defied all models to date. It is hoped that a more in depth study of the electron beam parameters may provide enough insight to enable a much improved understanding of the plasma focus in order to utilize the very promising features of this device as a compact pulsed accelerator. To this end, a prototype plasma focus accelerator has been designed and is under investigation. The prototype device, shown in Fig. 1(a), consists of a 15 microfarad, 20 kV capacitor connected to a transmission line through a spark gap switch. A Mather geometry plasma focus gun is placed at the end of the transmission line. The geometrical constraints imposed by the presence of the coaxial transmission line in our device require that we invert the usual plasma gun geometry in order to gain access to the electron beam which is accelerated down the middle of the hollow center electrode. The detail of this inverted geometry is shown in Fig. 1(b) and Ref. 8. In this electron beam mode of operation the capacitor bank is charged negatively, hence when the spark gap is triggered, a negative high voltage appears on the cathode in Fig. 1(b) causing breakdown across the pyrex insulator. We typically use 0.1-5 Torr Ar, He, N<sub>2</sub>, or H<sub>2</sub>, filling gas in the plasma gun region. After breakdown occurs, the plasma sheath is pushed toward the tip of the center electrode by magnetic pressure. Upon reaching the tip of the center electrode, the plasma current sheath collapses toward the axis. At this time, the plasma is unstable to  $m = 0$  sausage and  $m = 1$  kink modes. As pointed out in Ref. 11, the  $m = 0$  instability acts as an opening switch and a plasma diode. Electrons are accelerated down the center electrode and positive ions are accelerated in the opposite axial direction. The understanding of this plasma diode is crucial to the applications of the plasma focus device as a compact pulsed accelerator. It is the goal of this work to investigate the electron beam produced by this diode.

## II. Current Measurement

A Rogowski coil and a Faraday cup are used to measure the current exiting from the center electrode. The hollow center electrode acts as a gas filled drift region with inner diameter 14.3 mm and length 14.4 cm. The Rogowski coil consisting of 12 windings on a ring with a 35 mm diameter and a 9 mm<sup>2</sup> cross section is placed at the end of the center electrode drift region. The signal is integrated with a 875 ns (= RC) time constant. A major difficulty in using a Rogowski coil for current measurements is the fact that all current is measured, including plasma current induced by the beam as it passes through a gas filled region. In order to overcome this obstacle, a foil may be used to filter out the lower energy electrons which comprise the plasma current. High vacuum is maintained downstream of the foil to prevent another beam filling gas interaction.

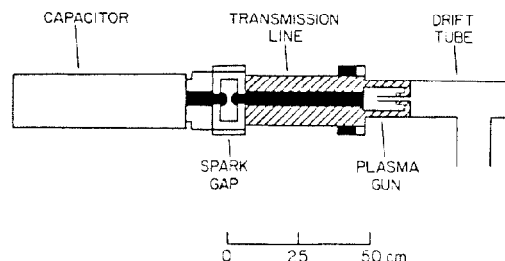


FIG. 1(a). Prototype plasma focus electron beam accelerator.

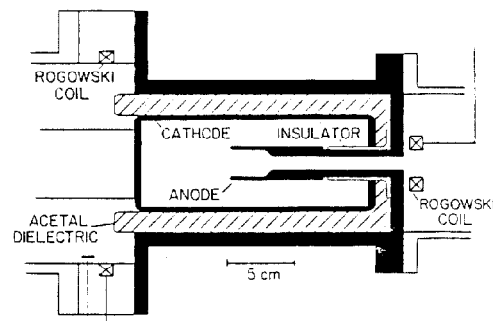


FIG. 1(b). Details of the inverted plasma gun geometry.

The Faraday cup is made of a 6.7 cm diameter, 1 cm thick graphite block connected to a 50 milliohm current viewing resistor. A foil is placed approximately 2 cm downstream of the end of the center electrode drift tube. Upstream of the foil, the ambient filling gas pressure is maintained, while

\*Work supported by the Air Force Office of Scientific Research, U.S. Department of Energy, and the Independent Research Fund at the Naval Surface Weapons Center.

<sup>a)</sup>Permanent address: Naval Surface Weapons Center, White Oak, Silver Spring, MD 20910

downstream a high vacuum ( $10^{-4}$  Torr) is maintained. Two different foils have been used: a  $6\text{ }\mu\text{m}$  mylar foil which effectively filters electrons with energies less than 20 keV, and a  $13\text{ }\mu\text{m}$  titanium foil which filters electrons with energies less than 60 keV. The graphite block is placed immediately (less than 1 cm) downstream of the foil in the vacuum region. Sample waveforms obtained from these diagnostics are shown in Fig. 2. Figure 2(a) is a waveform of a Rogowski coil taken with no foil and Fig. 2(b) is the Faraday cup signal with a  $13\text{ }\mu\text{m}$  foil. Notice the presence of plasma current in Fig. 2(a) which has a much longer time scale than the beam current in Fig. 2(b).

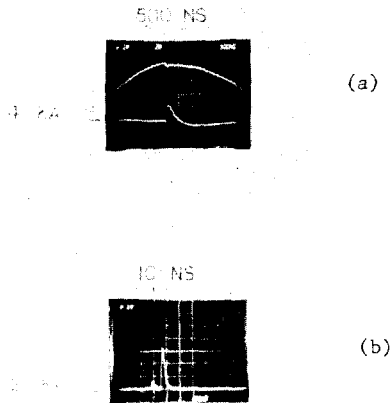


FIG. 2. (a) Waveform of an integrated Rogowski coil signal taken with no foil, (b) Current viewing resistor signal with a  $13\text{ }\mu\text{m}$  Ti foil.

### III. Energy Spectrum Measurements

A magnetic electron energy analyzer shown in Fig. 3 is used to determine the energy distribution of the electron beam. This simple analyzer is based upon particle deflection in a uniform magnetic field and utilizes the semicircular focusing principle. This diagnostic is described in detail in Ref. 12. A brief description will be given here for completeness. A uniform magnetic field region of 5.3 kGauss is provided by a rare earth cobalt permanent magnet enclosed in a soft iron case. The beam collimator consists of two slits separated by 35 mm. The upstream slit is  $125\text{ }\mu\text{m}$  wide and the downstream slit is  $25\text{ }\mu\text{m}$ . The relative energy resolution of the analyzer which results from these parameters is better than 2%. The electrons passing through the collimator are deflected in the magnetic field and follow a semicircular path to a phosphor detector. An open shutter photograph of the light emitted by the phosphor is used to record the information on a shot to shot basis. A microdensitometer scan of the exposed film provides more quantitative information. Figure 4 is a photograph of the phosphor during exposure to the electron beam produced by a 1 Torr Ar filling gas shot. Below is the microdensitometer scan of the film.

### IV. Emittance Measurements

A simple emittance meter<sup>13,14</sup> is used in the plasma focus device to measure the electron beam root-mean-square emittance. The meter is of a slit-pinhole design. It consists of a series of  $400\text{ }\mu\text{m}$  wide slits parallel to the y-axis upon which the beam is normally incident along the z-axis. An electron sensitive film is placed 4.32 mm downstream of the slits (see Fig. 5). After exposure the optical density of the film is scanned along  $y = 0$  with an optical densitometer. The scanning area of the densitometer defines the equivalent pinhole size. It

is convenient to use a film in which optical density is proportional to the exposure such as a radiachromic film.<sup>15</sup>

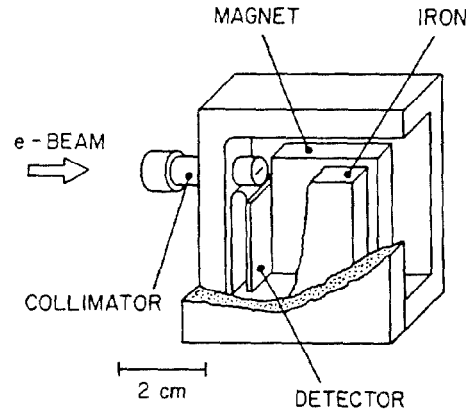


FIG. 3. A compact magnetic electron energy analyzer used to determine the energy distribution of the electron beam.

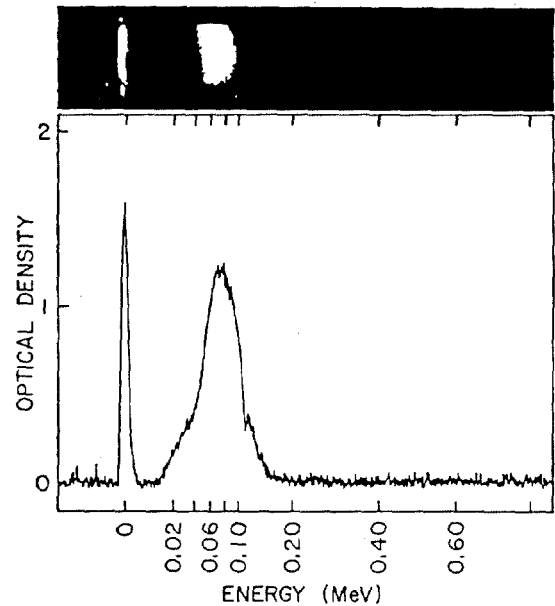


FIG. 4. Photograph of the phosphor during exposure to the electron beam produced by a 1 Torr Ar filling gas shot. Below is the microdensitometer scan of the film.

Reduction of the data entails several assumptions about the trace space  $(x, y, x', y')$  distribution of the beam.<sup>12</sup> We shall consider only axisymmetric beams, i.e. all measurable quantities are functions of  $r = \sqrt{(x^2 + y^2)}$  only. Also, zero beam rotation is assumed. In addition, we assume a thermal (Maxwellian) distribution in  $x' = dx/dz$  and  $y' = dy/dz$  space. Under these assumptions, the overall trace space distribution function  $f_4$  may be given by

$$f_4(x, y, x', y') = g(x, y) \exp -\left\{ \frac{(x' - \bar{x}')^2 + (y' - \bar{y}')^2}{2\sigma^2} \right\} g(x, y)$$

where  $g(x, y) = g(r)$  is x-y spatial dependence of the distribution function,  $\sigma(x, y) = \sigma(r)$  is the root-

mean-square value of the angle (velocity) in  $x'-y'$  space, and  $\bar{x}'(x,y)$  and  $\bar{y}'(x,y)$  are the mean angles in  $x'-y'$  space. For example, one source of a non-zero mean angle is overall beam divergence. Again these are in general functions of  $r$  only.

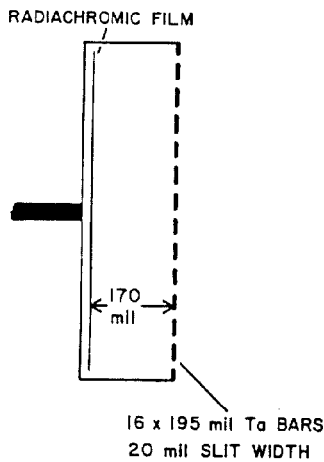


FIG. 5. Simple emittance meter used in the plasma focus device to measure the electron beam root-mean-square emittance. The meter is of a slit-pinhole design.

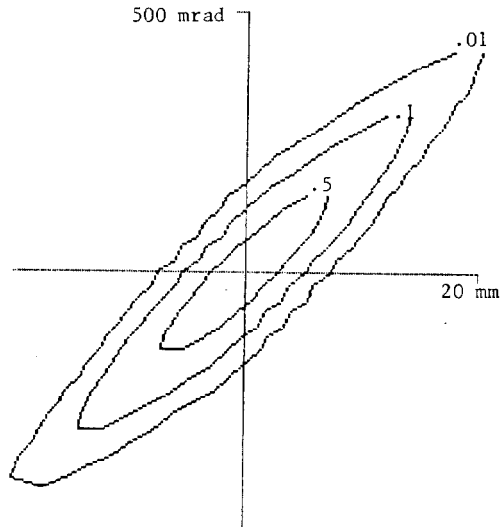


FIG. 6.  $f_2(x,x')$  contour plot projected on  $x-x'$  axes.

The microdensitometer scan along the  $y = 0$  line is used to find the functions  $g(x,y=0)$ ,  $\sigma(x,y=0)$  and  $\bar{x}'(x,y=0)$ . With these, axisymmetry determines the functions over full  $x-y$  space. Once these are determined,  $f_4$  is known, and with the assumption that the slit provides effective integral over  $y'$ , it is possible to integrate to obtain the mean values of  $x^2$  and  $x'^2$  and  $xx'$  which give the rms emittance as defined by Lapostolle<sup>16</sup> and Sacherer,<sup>17</sup>

$$\epsilon_{\text{rms}} = 4[\langle x^2 \rangle \langle x'^2 \rangle - \langle xx' \rangle^2]^{1/2}.$$

We will now describe the methods by which  $g(x,y=0)$ ,  $\sigma(x,y=0)$  and  $\bar{x}'(x,y=0)$  are obtained from the scan. Each slit selects a certain  $x$  within the

beam say  $x_i$ . The peak on the detector corresponding to the  $x_i$  slit exhibits a characteristic height, rms width, and position. With the assumption of Maxwellian distribution as discussed above, the half width half maximum of the peak is just  $\sqrt{(2 \ln 2)}$  times  $\sigma(x_i,0)L$  where  $L$  is the distance from slit to detector. By fitting these to a smooth function  $\sigma(x,0)$  is obtained. The mean position of the peak  $\bar{x}_i$  relative to its position for a beam in which all trajectories are parallel to the axis, gives  $\bar{x}'(x_i,y=0)L$ . These are fit to a straight line as is expected for a uniformly diverging beam to find  $\bar{x}'(x,y=0)$ .  $g(x_i,0)$  is just the integral of the individual distribution. Connecting these with a smooth function gives  $g(x,0)$ .

The emittance meter is placed immediately downstream of the hollow center electrode and exposed. The radiachromic film is scanned with a microdensitometer and analyzed in the above manner. Figure 6 shows a contour plot of

$$\iint f_4(x,y,x',y') dy dy' = f_2(x,x').$$

The rms emittance at the beam port is found to be 1288 mm-mrad.

#### V. Acknowledgment

The authors gratefully acknowledge useful discussions with W. Namkung.

#### VI. References

1. R. L. Gullickson and R. H. Barlett, *Adv. X-Ray Anal.* **18**, 184 (1975).
2. W. L. Harris, J. H. Lee, and D. R. McFarland, *Plasma Phys.* **20**, 95 (1978).
3. J. H. Lee, "Electron Beam Generation and Laser Excitation by Plasma Focus Discharges," in *Proceedings of 2nd Int. Workshop on Plasma Focus*, (Moscow, 1981), p. 196.
4. V. Nardi, W. H. Bostick, J. Feugeas, W. Prior, and C. Cortese, "Energy Spectra of Deuteron and Electron Beams from Focused Discharges and Optimization Criteria," in *Proceedings of 7th Int. Conf. on Plasma Physics and Controlled Nuclear Fusion Research*, (Innsbruck, 1978), p. 143.
5. M. Yokoyama, Y. Kitagawa, Y. Yamada, C. Yamanaka, and K. Hirano, "Recent Progress in Dense Plasma Focus," in *Proceedings of 8th Int. Conf. on Plasma Physics and Controlled Nuclear Fusion Research*, (Brussels, 1979), p. 187.
6. W. Stygar, G. Gerdin, F. Venneri, and J. Mandrekas, *Nucl. Fusion* **22**, 1161 (1982).
7. W. Neff, H. Krompholz, F. Rühl, K. Schönbach, and G. Herziger, *Phys. Lett.* **79A**, 165 (1980).
8. J. R. Smith, C. M. Luo, M. J. Rhee, and R. F. Schneider, "Operation of a Plasma Focus Device as a Compact Electron Accelerator," to be published in *Phys. Fluids*, July 1985.
9. J. W. Mather, *Methods of Experimental Physics*, (Academic Press, New York, 1971), pp. 187-249.
10. P. G. Eltgroth, *Phys. Fluids* **25**, 2408 (1982).
11. M. J. Rhee and R. F. Schneider, *IEEE Trans. Nucl. Sci.* **NS-30**, 3192 (1983).
12. R. F. Schneider, C. M. Luo, M. J. Rhee, and J. R. Smith, "A Compact Magnetic Electron Energy Analyzer," submitted to *Rev. Sci. Instrum.*
13. J. R. Smith, W. Namkung, M. J. Rhee, and H. S. Uhm, *Bull. Am. Phys. Soc.* **29**, 1274 (1984).
14. J. R. Smith, et al., paper at this conference.
15. K. C. Humphreys and A. D. Kantz, *IEEE Trans. Nucl. Sci.* **NS-26**, 1784 (1979).
16. P. M. Lapostolle, *IEEE Trans. Nucl. Sci.* **NS-18**, 1101 (1971).
17. F. J. Sacherer, *IEEE Trans. Nucl. Sci.* **NS-18**, 1105 (1971).